Fluorescence measurements of the exciton dispersion in $Gd(OH)_3$

Y. Salem and B. Jacquier
Université Lyon I, 69622 Villeurbanne, France

R. L. Cone
Physics Department, Montana State University, Bozeman, Montana 59717

(Received 6 June 1989; revised manuscript received 2 October 1989)

We report an observation of the intrinsic fluorescence of $Gd(OH)_3$ arising from exciton band-to-band transitions occurring primarily at the edge of the Brillouin zone. Using the ${}^8S_{7/2}$, $M_J=-\frac{5}{2}$, magnon dispersion, we found an exciton dispersion of 1.8 cm^{-1} for the ${}^6P_{7/2}$, $M_J=-\frac{7}{2}$ crystal state at 2 K in an applied magnetic field of 35 kG. Transitions involving the second excited spin state of the ground manifold have also been observed in absorption and emission. In contrast to the magnon state, the $M_J=-\frac{3}{2}$ state has little or no dispersion. By time resolving the emission, it is clear that the relaxation of the initially excited $k=0$ excitons to k values at the zone edge takes place faster than 10 nsec.

I. INTRODUCTION

Optical excitations of the localized electrons of transition-metal and rare-earth magnetic insulators may be described in terms of strongly coupled electron-hole pairs called Frenkel excitons. Exciton band dispersion has been illustrated for several concentrated rare-earth materials (a) by means of absorption line shape analysis in $GdCl_3$ (Refs. 1 and 2) and $Gd(OH)_3$ (Ref. 1), and (b) by light scattering in $PrAlO_3$ (Ref. 3) and $TbVO_4$.[4] To our knowledge, only the investigations on $Tb(OH)_3$ (Refs. 5 and 6) have considered the fluorescence properties of the rare-earth exciton bands by analyzing the emission line shape of the band-to-band transition and by looking at the fluorescence dynamics at a short time after selective laser pulse excitation. These considerations are of prime importance in the elucidation of the problem of energy migration in rare-earth materials where the nature of both ion-ion interactions and electronic states is still a wide open field of investigation.[7]

In this article we describe the observation of fluorescence transitions ${}^6P_{7/2}$ ($M_J=-\frac{7}{2}$) to ${}^8S_{7/2}$ ($M_J=-\frac{7}{2}$, $-\frac{5}{2}$, $-\frac{3}{2}$) of $Gd(OH)_3$ for an external magnetic field applied along the c axis of the crystal at 2 K. First, we shall describe the basic physical situation by summarizing the general fluorescence properties of $Gd(OH)_3$, then we shall analyze the detailed structure of the excitation (or absorption) spectra of the ${}^8S_{7/2}\rightarrow{}^6P_{7/2}$ transition, and finally, we shall discuss the fluorescence dynamics recorded at high magnetic field.

II. EXPERIMENTAL DETAILS

$Gd(OH)_3$ has the well-known hexagonal structure observed for the entire series of the rare-earth hydroxides with space group $P6_3/m$ (C_{6h}^2). The Gd^{3+} ions occupy sites of C_{3h} symmetry and are each surrounded by two Gd^{3+} nearest neighbors along the c axis and six next-nearest neighbors in triangles above and below, as shown in Fig. 1(a). It has been shown[8] that $Gd(OH)_3$ orders antiferromagnetically at 0.94 K with predominant nearest-neighbor interactions; however, in an external magnetic field, the Gd^{3+} spins can be aligned along the field, providing an aligned paramagnetic spin configuration similar to that of a ferromagnet. That aligned state has the sim-

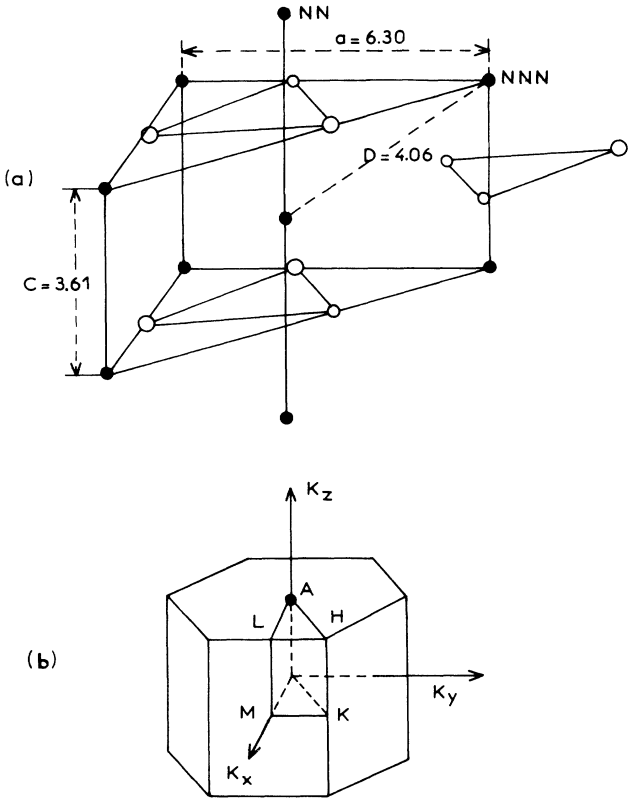

FIG. 1. Crystal structure (a) and first Brillouin zone (b) for $Gd(OH)_3$ crystal.

plest exciton band picture, and it is thus emphasized in our experiments.

A needlelike $Gd(OH)_3$ single crystal was used with an optical path of the order of 0.3 mm perpendicular to the needle and c axes. It was immersed in a pumped helium bath providing a temperature of approximately 2 K. Selective laser excitation was achieved by frequency-doubled pulses from a neodymium YAG-pumped laser. The potassium dihydrogen phosphate (KDP) doubling crystal was automatically optimized for each wavelength, allowing computerized scanning of the excitation or absorption spectra. A Jobin-Yvon U-1000 double monochromator working in second order was used to analyze the fluorescence with a resolution better than 1 cm^{-1} in the uv range. Single photon counting ensured a good signal to noise ratio. Further experimental details will be presented elsewhere.[9]

III. RESULTS AND DISCUSSION

Figure 2 schematically shows the $^8S_{7/2}$ ground state and $^6P_{7/2}$ excited state of $Gd(OH)_3$. Laser excitation in one of the upper $^6P_{7/2}$ Stark components induces an intense uv fluorescence which is composed of several sharp lines ranging from 32 024.6 cm^{-1} to 31 830 cm^{-1} at the temperature of 2 K. All of these lines, except the one at 32 024.6 cm^{-1}, which is resonant with the lowest Stark component of the $^6P_{7/2}$ state (seen in absorption), are attributed to impurity-induced Gd^{3+} trap emission[9] which is well known in concentrated rare-earth materials.[10] For the sample used in this study, the resonant fluorescence line (often called intrinsic) is isolated from the traps by more than 60 cm^{-1}. Furthermore, no unidentified excitation lines are detected near the resonance which could result from direct excitation of traps. This gives one significant confidence to make a detailed analysis of the intrinsic emission and excitation profiles. Before analyzing the fluorescence data, we note that the exact number of absorption lines expected from the splitting of both $^6P_{7/2}$ and $^8S_{7/2}$ states in an applied magnetic field have been observed in the one-[9] and two-photon[11] polarized excitation spectra at 2 K and they all obey the selection rules for one- and two-photon absorption processes. Further, those results agree well with earlier one-photon absorption data by Meltzer and Moos,[1] who initially demonstrated the influence of the magnon and exciton dispersion on the positions and line shapes of single-ion-induced rare-earth optical transitions. The simplest exciton band applies to $Gd(OH)_3$ in the aligned paramagnetic state with all ground state spins oriented parallel to the c axis.[1,12] In a strong applied magnetic field, that picture is appropriate.

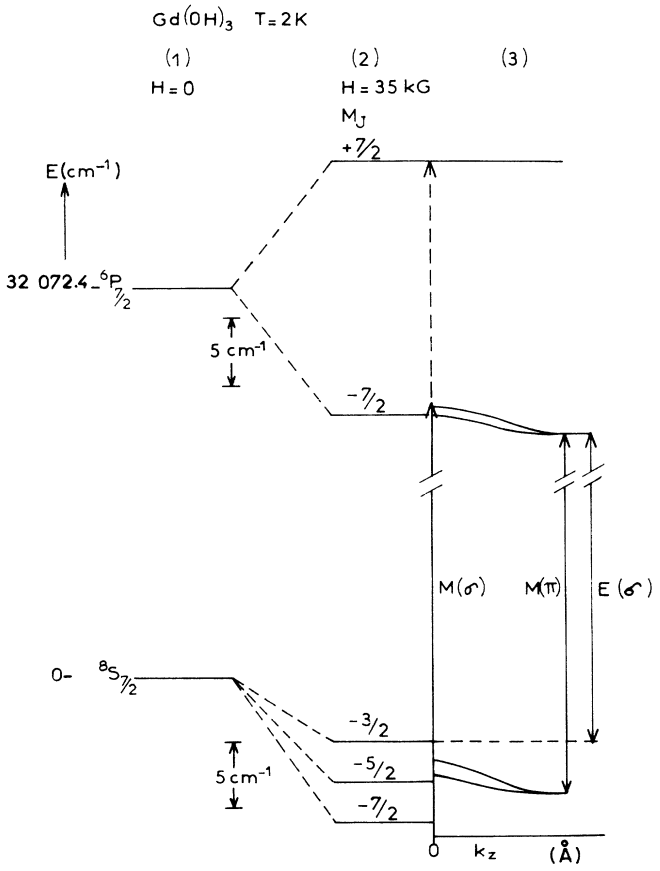

FIG. 2. Schematic electronic energy levels involved in the optical transitions for $Gd(OH)_3$ (1) at zero field, (2) at 35 kG, and (3) introducing a simplified energy dispersion with respect to k_A.

A. Basic spectroscopy of the $^8S_{7/2}$ ground state and $^6P_{7/2}$ exciton bands

In Fig. 3, we have reported the emission and polarized excitation spectra at 2 K in a 35 kG magnetic field. A standard mercury line was used to calibrate the monochromator for the emission and to control the laser wavelength. The σ-polarized excitation spectrum (dashed line) exhibits a strong $^8S_{7/2}$, $M_J=-\frac{7}{2}$ to $^6P_{7/2}$, $M_J=-\frac{7}{2}$ pure $k=0$ exciton line, whose excitation profile varies substantially with pumping intensity (the sample is optically thick for that transition). In the π-polarized spectrum (dotted line), that excitation line is very small compared to a new $^8S_{7/2}$, $M_J=-\frac{5}{2}$ to $^6P_{7/2}$, $M_J=-\frac{7}{2}$ magnon-to-exciton line peaking at 3.9 cm^{-1} to lower energy. The unpolarized intrinsic fluorescence spectrum (solid line) was excited by pumping an upper electronic component of $^6P_{7/2}$. The fluorescence reproduces remarkably well both the peak positions and the line profile of the π-polarized excitation spectrum with an additional weak and asymmetrical $^8S_{7/2}$, $M_J=-\frac{3}{2}$ line peaking at 8 cm^{-1} from the first line. The two high energy excitation lines at 0 and 3.9 cm^{-1} agree with the previous results of Meltzer and Moos[1] who measured the same energy difference and the width of 1.1 cm^{-1} for the low energy line (at 3.9 cm^{-1}). These excitation lines have been attributed, respectively, to the $k=0$ pure electronic transition $^8S_{7/2}$, $M_J=-\frac{7}{2}$ to $^6P_{7/2}$, $M_J=-\frac{7}{2}$ and to the band-averaged magnon-to-exciton transition from the first thermally populated spin state $^8S_{7/2}$, $M_J=-\frac{5}{2}$ to $^6P_{7/2}$, $M_J=-\frac{7}{2}$.

The central part of Fig. 2 represents the theoretical

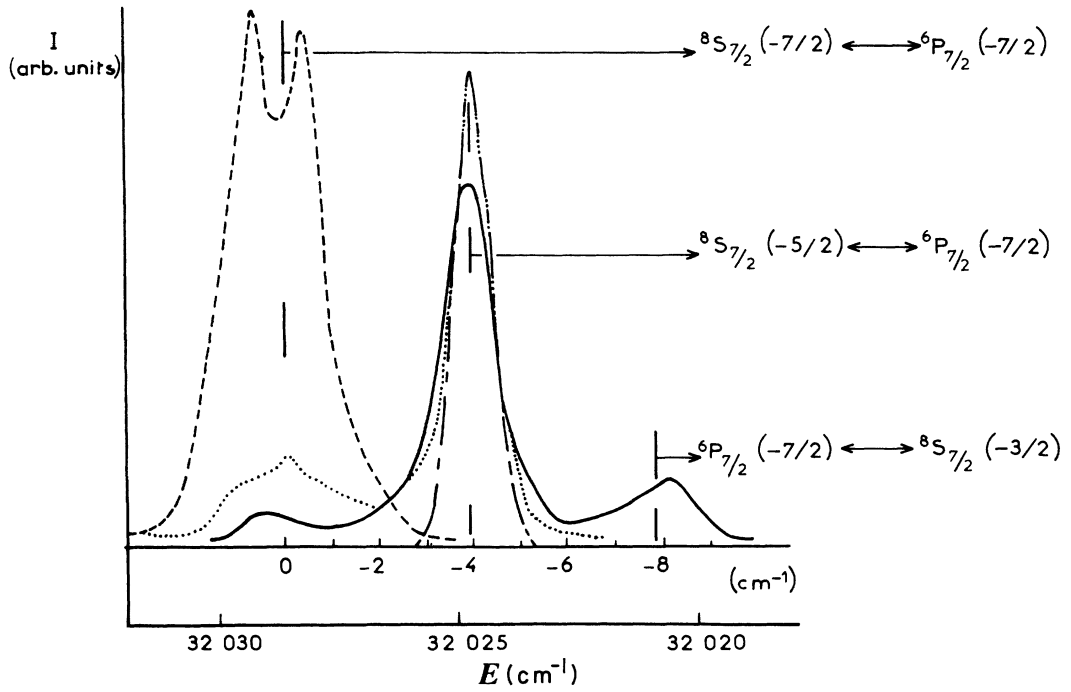

FIG. 3. Excitation and fluorescence spectra for $^8S_{7/2}$ to $^6P_{7/2}$ transitions of $Gd(OH)_3$ at 2K and $H=35$ kG with the field applied along the c axis; the unpolarized intrinsic fluorescence spectrum (solid line), and π (dotted line), and σ (dashed line) polarized excitation spectra of the trap fluorescence. Laser resolution was 0.1 cm^{-1}, and monochromator resolution was 0.6 cm^{-1}. Theoretical fit of the excitation line profile (from $^8S_{7/2}$, $M_J=-\frac{5}{2}$) is represented by the dot-dashed line after Ref. 9.

Zeeman splitting of the observed transitions calculated with the g factors of 2 and 1.71 for the ground and excited states, respectively. In agreement with Meltzer's model,[1] the observed transitions are represented on the right hand side of Fig. 2 where a very simplified band structure of the ground and excited states along the k_z direction [Fig. 1(b)] is included. Further calibration of the peak positions corresponding to the vertical bars was ensured by the presence of the $k=0$ pure electronic transition $^8S_{7/2}$, $M_J=-\frac{7}{2}$ to $^6P_{7/2}$, $M_J=+\frac{7}{2}$, the forbiddenness of which is relaxed by the small admixture of $M_J=+\frac{7}{2}$ and $-\frac{5}{2}$.[1] The shift of that $M_J=+\frac{7}{2}$ line with the magnetic field (at least for high fields) agrees with the theoretical Zeeman splitting. We note that this calibration is fully redundant with the calibration of the fluorescence spectrum using the standard mercury line. These observations further confirm the position of the $k=0$ pure electronic transition to the $^6P_{7/2}$, $M_J=-\frac{7}{2}$ on the upper exciton branch.[1,12]

The difference in energy of the absorption lines for the $k=0$ transition from the ground state and the band-averaged transition from the thermally populated magnon state to the $^6P_{7/2}$, $M_J=-\frac{7}{2}$ exciton arises from a combination of the Zeeman splittings of the ground and excited states and the ion-ion interactions. The interactions contribute both splittings and exciton dispersion.[1,7,12] Knowledge of the magnon dispersion allowed Meltzer and Moos[1] to deduce the exciton dispersion from the absorption line shapes. Their analysis showed that the band-averaged absorption at low temperature involves predominantly zone-boundary magnons, so the effects of exciton dispersion are primarily evident as *shifts* in line positions. At low temperature, the absorption transitions remain relatively narrow and are not too asymmetric. This is clearly true for our excitation data as well.

We now consider the fluorescence spectrum which was excited by pumping an upper electronic component of $^6P_{7/2}$. The fluorescence spectrum is independent of the specific $^6P_{7/2}$ component used for excitation. We assume that the nonradiative relaxation process and subsequent exciton scattering processes result in a quasi-thermal-equilibrium distribution of the exciton k vectors in the $^6P_{7/2}$, $M_J=-\frac{7}{2}$ band. As we shall see, the exciton scattering time across the Brillouin zone is shorter than the fluorescence lifetime (few μs) so that process alone would result in the assumed condition. Fluorescence thus occurs with $\Delta k\simeq 0$ for all $\mathbf{k}$ vectors giving the so-called band-average transition, but the large dispersion in conjunction with the low temperature results in a quasiequilibrium population of predominantly zone-boundary excitons. Figure 3 shows that there is exciton-to-magnon fluorescence intensity all across the Brillouin zone. The strong peak at 3.9 cm^{-1} is a consequence of the favored zone-boundary population.

In summary, under quasiequilibrium conditions, the fluorescence and excitation line profiles of the transition $^8S_{7/2}$, $M_J=\frac{5}{2}$ to $^6P_{7/2}$, $M_J=-\frac{7}{2}$ are similar. A full theoretical analysis of the fluorescence line shape involving the thermally weighted exciton density of states will be published later,[9] which confirms the previous determination of an exciton dispersion of 1.8 cm^{-1}.[1]

The weak broad line peaked at 8 cm^{-1} lower than the $k=0$ transition is a new feature of the fluorescence spectrum and as we shall see, it provides an independent determination of the ${}^6P_{7/2}$, $M_J=-\frac{7}{2}$ exciton dispersion. This feature is attributed to the destruction of one ${}^6P_{7/2}$, $M_J=-\frac{7}{2}$ exciton and the excitation of a highly excited spin state $M_J=-\frac{3}{2}$ both of wave vector **k**. The observed line shape again involves an average over the entire Brillouin zone,[1,12] but the nature of the lower state is quite different. Taking account of the level splittings in the ground state ($M_J=-\frac{3}{2}$) and excited state ($M_J=-\frac{7}{2}$) but ignoring the exciton dispersion, this transition would be expected at 6 cm^{-1} from the pure $k=0$ electronic transition. The difference between 6 cm^{-1} and the measured peak value of 8 cm^{-1} can be attributed primarily to the exciton dispersion. (As for the exciton-to-magnon band-averaged transition which we considered above, the low temperature fluorescence to the $M_J=-\frac{3}{2}$ spin state involves primarily an initial state quasiequilibrium population of zone-boundary excitons.) After careful analysis of transitions involving absorption to the higher crystal-field state (${}^8S_{7/2}$, $M_J=-\frac{7}{2}$ to ${}^6P_{7/2}$, $M_J=-\frac{3}{2}$) and absorption from the second excited spin state [${}^8S_{7/2}$, ($M_J=-\frac{3}{2}$) to ${}^6P_{7/2}$ ($M_J=-\frac{3}{2}$)], almost zero dispersion is deduced for the spin state ${}^8S_{7/2}$, $M_J=-\frac{3}{2}$. An upper limit of 0.2 cm^{-1} can be estimated. Indeed, a small ${}^8S_{7/2}$, $M_J=-\frac{3}{2}$ dispersion is expected theoretically, since the coupling of two Gd^{3+} ions involves $\Delta S=2$ which should make it very weak, leading to a very small dispersion.[1,7,12] This is theoretically related to the analogously weak dispersion of the excited state ${}^6P_{7/2}$, $M_J=-\frac{3}{2}$.[1,9,12] The fluorescence line attributed to the transition, from ${}^6P_{7/2}$ ($M_J=-\frac{7}{2}$) to ${}^8S_{7/2}$ ($M_J=-\frac{3}{2}$), thus involves almost no magnon dispersion, and consequently, its position directly reveals the strong exciton dispersion of the excited state ${}^6P_{7/2}$, $M_J=-\frac{7}{2}$. We thus find additional evidence of the collective nature of the optical excitation of the ${}^6P_{7/2}$ manifold of $Gd(OH)_3$.

B. ${}^6P_{7/2}$ exciton dynamics

As an important extension of the static spectroscopic analysis described above, we were able to look at the dynamics of the fluorescence following preparation of the system in a nonequilibrium $k=0$ crystal state at 2 K and $H=35$ kG. A 10 nsec laser pulse was used to excite the pure $k=0$ electronic transition ${}^8S_{7/2}$, $M_J=-\frac{7}{2}$ to ${}^6P_{7/2}$, $M_J=-\frac{7}{2}$, and the monochromator was set at the wavelength of the exciton-to-magnon transition. The spectral resolution combined with good stray light rejection at short times provided a clear wave-vector-selective analysis[5,6,13] of the fluorescence. A fast digital oscilloscope allowed us to detect an initial rise of the fluorescence similar to that of the laser pulse. This means that the relaxation of excitons across the Brillouin zone occurs within a time scale faster than 10 nsec, a result which is not surprising due to the strong dispersion of the excited state. A further experiment where the laser was set at the magnon-exciton transition and the monochromator at the $k=0$ transition exhibits the same behavior.

IV. SUMMARY AND CONCLUSION

By using new transitions in laser-induced fluorescence experiments, we have extended the exciton band studies of $Gd(OH)_3$ of Meltzer and Moos.[1] Our observations of band-averaged exciton-to-magnon transitions at 2 K confirmed the 1.8 cm^{-1} exciton dispersion of the ${}^6P_{7/2}$, $M_J=-\frac{7}{2}$ band in the aligned paramagnetic state. In addition, we found that the second excited spin state had a nominally "flat" dispersion as expected, and band-averaged transitions to that state allowed a second confirmation of the ${}^6P_{7/2}$, $M_J=-\frac{7}{2}$ exciton band dispersion.

Time resolved fluorescence experiments allowed observation of wave-vector-selective exciton dynamics which cannot be observed in absorption experiments. We found that there is very fast scattering of excitons both from $k=0$ states to the Brillouin zone boundary and from the zone boundary to the zone center ($k=0$) under the conditions of our experiments.

ACKNOWLEDGMENTS

The authors wish to thank Professor W. P. Wolf and Dr. S. Mroczkowski of Yale University for providing us with the $Gd(OH)_3$ single crystals and Dr. R. Mahiou and Dr. R. S. Meltzer for helpful discussions. The Universite Lyon I is Unite Associeé No. 442 du Centre Nationale de la Recherche Scientifique.

[1] R. S. Meltzer and H. W. Moos, Phys. Rev. B **6**, 264 (1972).
[2] R. Mahiou, B. Jacquier, and R. Moncorgé, *Procceedings of the Rare Earth Symposium* (World Scientific, Singapore, 1984).
[3] R. J. Birgeneau, J. K. Kjems, C. S. Shirane, and L. G. Van Uitert, Phys. Rev. B **10**, 2512 (1974).
[4] H. B. Ergun, K. A. Gehring, and G. A. Gehring, J. Phys. C **9**, 1101 (1976).
[5] R. L. Cone and R. S. Meltzer, J. Chem. Phys. **62**, 3575 (1975).
[6] R. S. Meltzer, Solid State Commun. **20**, 553 (1976); H. T. Chen and R. S. Meltzer, Phys. Rev. Lett. **44**, 599 (1980).
[7] R. L. Cone and R. S. Meltzer, in *Spectroscopy of Rare Earth Ions in Crystals,* edited by A. A. Kaplyanskii and R. M. Macfarlane (North-Holland, Amsterdam, 1987), pp. 481–556.
[8] A. T. Skjeltorp, C. A. Catanese, H. F. Meissner, and W. P. Wolf, Phys. Rev. B **7**, 2062 (1972).
[9] Y. Salem, B. Jacquier, R. Mahiou, and R. L. Cone (unpublished).
[10] M. F. Joubert, B. Jacquier, R. Moncorgé, and G. Boulon, J. Phys. **43**, 893 (1982).
[11] B. Jacquier, Y. Salem, C. Linarès, J. C. Gâcon, R. Mahiou, and R. L. Cone, J. Lumin. **38**, 258 (1987); **38**, 260 (1987).
[12] R. L. Cone and R. S. Meltzer, Phys. Rev. Lett. **18**, 859 (1973); R. S. Meltzer and R. L. Cone, Phys. Rev. B **13**, 2818 (1976).
[13] First application of this wave-vector-selective technique was made by R. M. Macfarlane and A. C. Luntz, Phys. Rev. Lett. **31**, 832 (1973).